Marine Pollution Bulletin 103 (2016) 115–127

Contents lists available at ScienceDirect

Marine Pollution Bulletin

journal homepage: www.elsevier.com/locate/marpolbul

Regional approach to modeling the transport of floating plastic debris in the Adriatic Sea

S. Liubartseva [a,*], G. Coppini [b], R. Lecci [b], S. Creti [b]

[a] Centro EuroMediterraneo sui Cambiamenti Climatici, Bologna, Italy
[b] Centro EuroMediterraneo sui Cambiamenti Climatici, Lecce, Italy

ARTICLE INFO

Article history:
Received 12 November 2015
Received in revised form 18 December 2015
Accepted 21 December 2015
Available online 8 January 2016

Keywords:
Plastic debris inputs
Lagrangian model
Markov chain
Plastic fluxes onto coastline
Impact matrices

ABSTRACT

Sea surface concentrations of plastics and their fluxes onto coastlines are simulated over 2009–2015. Calculations incorporate combinations of terrestrial and maritime litter inputs, the Lagrangian model MEDSLIK-II forced by AFS ocean current simulations, and ECMWF wind analyses. With a relatively short particle half-life of 43.7 days, the Adriatic Sea is defined as a highly dissipative basin where the shoreline is, by construction, the main sink of floating debris. Our model results show that the coastline of the Po Delta receives a plastic flux of approximately 70 kg(km day)$^{-1}$. The most polluted sea surface area (>10 g km^{-2} floating debris) is represented by an elongated band shifted to the Italian coastline and narrowed from northwest to southeast. Evident seasonality is found in the calculated plastic concentration fields and the coastline fluxes. Complex source–receptor relationships among the basin's subregions are quantified in impact matrices.

1. Introduction

Plastic pollution in the marine environment is of increasing concern due to the great threat to human health and the stability of marine ecosystems, and adverse economic impacts on coastal communities (Eriksen et al., 2014; Thompson et al., 2009).

The spatial and temporal distributions of plastics in the marine environment depend on input locations and the time-varying intensity of sources, which are highly uncertain. However, ocean currents, waves, and wind control the transport of plastics, redistributing them at sea until they eventually wash ashore or sink. The high complexity and multiscale versatility of the dynamics of the upper mixed layer of the ocean, where the majority of plastics float, must be taken into account.

In order to identify the pathways of floating marine litter under such uncertain conditions, several numerical simulations were performed for different geographical areas varying from global to regional scales. Contributions of geostrophic currents, Ekman drift, Stokes drift, and their combinations in the North Pacific were simulated by Kubota (1994). Developing Kubota's approach, Martinez et al. (2009) demonstrated the appropriateness of using a high-resolution current field to determine the impact of mesoscale activity on the trajectories of particles. Yoon et al. (2010) enriched the methodology, switching from homogeneous source distribution to more realistic inputs into the Japan Sea from the largest cities and rivers, applying output from the Japan Sea Forecasting System.

Remarkable progress toward flexibility in plastic litter modeling was achieved by Maximenko et al. (2012), who suggested a Markov chain model that represents transporting properties of the upper mixed layer, allowing the separation of the input distributions from the dynamics of the upper mixed layer. Once the Markov chain model was built, the evolution of particle concentration from any source could be calculated, and various hypotheses of input distributions could be tested efficiently. A global set of historical trajectories of drifting buoys deployed in the Surface Velocity Program and Global Drifter Program (1979–2007) was used for the calculation of a transition matrix. The methodology was improved by van Sebille et al. (2012), who extended the buoy dataset, introduced the seasonal transition matrices, and imposed marine litter inputs related to the coastal population density.

Using directly integrated particle trajectories, Lebreton et al. (2012) took into account terrestrial sources from rivers and cities, and marine inputs from major shipping lanes. Long-term drift of floating debris in the world's oceans was simulated assuming an increase in input intensity.

Recently, marine plastic modeling was carried out on a regional scale to explain local source–receptor relationships in the southern North Sea (Neumann et al., 2014). In the Mediterranean Sea, marine litter drift was simulated in an effort to find permanent accumulation structures such as so-called garbage patches (Mansui et al., 2015). No permanent sea surface structures able to retain floating items in the long-term were found. However, some relevant coastal features were obtained at a basin scale. For example, the coastline between Tunisia and Syria was found to be the most littered with plastics, while the western Mediterranean demonstrated rather low coastal impact.

* Corresponding author.
E-mail address: svitlana.liubartseva@cmcc.it (S. Liubartseva).

http://dx.doi.org/10.1016/j.marpolbul.2015.12.031
0025-326X/

Assuming that marine litter particles can be considered passive Lagrangian tracers, it is important to mention Pizzigalli et al. (2007), who, for the first time, built a Markov chain model for passive tracers in the Mediterranean Sea using the Lagrangian model coupled with the Mediterranean Forecasting System (Pinardi et al., 2003). They focused on seasonality in calculated statistics and introduced coastal-approach-maps to find coastlines that are at risk of pollution originating from the sea.

To a certain extent, transport of plastic marine litter is similar to the transport of satellite-tracked Lagrangian drifters, which have been intensively deployed in the Adriatic Sea. The results obtained in the drifter experiments conducted by Falco et al. (2000), Poulain (2001) Lacorata et al. (2001), Ursella et al. (2006), Veneziani et al. (2007), Poulain and Hariri (2013) were invaluable for verification of model results on distribution of floating debris in the Adriatic Sea.

Focusing on a key role of uncertainty in the plastic debris inputs, Isobe et al. (2009) tried to reconstruct sources of plastic debris solving an inverse problem (backtracking). The main complication of this problem arose from the irreversibility of diffusion computed using the random-walk technique (Csanady, 1973). Recently, when microplastics became widely recognized as an acute problem, 3D modeling was developed for meso- and micro-plastics (Isobe et al., 2014). Some relevant parameters in floating debris modeling, which are comparable with those we use in our calculations, are extracted from the literature cited and summarized in Table 1.

In the present work, for the first time we (1) develop the Markov chain model based on coupling the Lagrangian MEDSLIK-II model (De Dominicis et al., 2013a,b) with the Adriatic Forecasting System (AFS) ocean currents simulations and ECMWF surface wind analyses to simulate the plastic concentrations at the sea surface and fluxes onto the coastline that originated from terrestrial and maritime inputs; (2) identify source–receptor relationships among the subregions of the Adriatic Basin solving both the direct and inverse problems; and (3) present the results in terms of impact matrices.

The manuscript is organized as follows: in Section 2 the data on sources of floating debris in the Adriatic Sea, the Lagrangian model, and the ocean forecasting system are presented; Section 3 contains descriptions of the Markov chain model; and Section 4 presents results and discussion. Finally in Section 5, we draw conclusions.

2. Data and models

2.1. Identification of floating debris inputs into the Adriatic Sea

According to recent estimations by Jambeck et al. (2015), the total annual input of plastic in the Adriatic Sea was 10,000–250,000 tons in 2010. In an effort to be more consistent with the previous estimates of the mass of floating plastic debris cited in Jambeck et al. (2015) we use a lower limit of 10,000 ton year $^{-1}$ in the present work. Following Lebreton et al. (2012), we assume that 40% of the marine litter enters the basin through rivers; 40% through coastal urban populations; and the remaining 20% is derived from shipping lanes. They yield 4000, 4000, and 2000 ton year $^{-1}$, respectively.

Average annual discharges into the Adriatic Basin from the 62 largest rivers are extracted from a database implemented by Verri et al. (2014). The discharge of the Po River is distributed among its nine greatest distributaries in proportion to their respective runoffs. Eight rivers entering the north Ionian Sea are included in order to take into consideration

Table 1
Relevant parameters in floating plastic debris modeling.

Domain, reference	Meteo-oceanographic data	Distribution of inputs		Interaction with coastline	Number of Lagrangian particles	Time of integration
		Spatial	Temporal			
North Pacific (Kubota, 1994)	COADS climatology (1970–1979)	10°×10° homogeneous grid	Instantaneous release	No-slip conditions	50	5 years
South Pacific (Martinez et al., 2009)	OSCAR based currents (1993–2001)	1°×1° homogeneous grid	Instantaneous release	No-slip conditions	Large number, not specified	8 years (1993–2001)
East China Sea (Isobe et al., 2009)	Quick scatterometer wind and POM based currents	Two point sources	Instantaneous release	Beaching after 12-h stagnation	20000	76 days
Japan Sea (Yoon et al., 2010)	Currents based on Japan Sea Forecasting System (2003–2006)	Inputs from largest basin's rivers, cities and, the Tsushima Strait	Every month release (2003–2006)	Beaching	47676 particles a year	4 years (2003–2006)
Mediterranean Sea (Pizzigalli et al., 2007)	Lagrangian model dataset based on currents provided by Mediterranean Forecasting System (2000–2004)	1/8°×1/8° homogeneous grid	Every week release (2000–2004)	No-slip conditions	In the Markov chain model: 400000 particles a week	28 days
Global ocean (Maximenko et al., 2012)	Lagrangian dataset of satellite-tracked drifting buoys (1979–2007)	1/2°×1/2° homogeneous grid	Instantaneous release	Beaching after 5-day stagnation	In the Markov chain model: large number, not specified	10 years
Global ocean (van Sebille et al., 2012)	Lagrangian dataset of drogued and non-drogued drifting buoys (198x–20xx)	Inputs from coastal urban population	6 pulse releases a year	No-slip conditions	In the Markov chain model: large number, not specified	1000 years
Global ocean (Lebreton et al., 2012)	6-year dataset provided by US Navy's Global Atmospheric Prediction System and HYCOM/NCODA ocean circulation model	Inputs from impervious surface area, coastal population and shipping lanes	Releases evenly distributed over each year	Beaching	Over 9.6×10^6	30 years
Southern North Sea (Neumann et al., 2014)	BSHcmod: operational weather and ocean circulation models	Two local clusters with homogeneous distributions inside	One release in 28 h (2000–2008)	No-slip conditions	200	90 days
Mediterranean Sea (Mansui et al., 2015)	NEMO based currents	10×10 km homogeneous grid	Everyday release (2001–2009)	Beaching, stagnation, recirculation off shore	3287	Two runs: one year and 3 months
Adriatic Sea (present work)	Lagrangian model dataset based on ECMWF wind and AFS currents (2009–2015)	Inputs from largest Adriatic rivers, cities and shipping lanes	One release in 10 days (2009–2015)	Beaching after 10-day stagnation	In the Markov chain model: over 6×10^{10}	6 years (2009–2015)

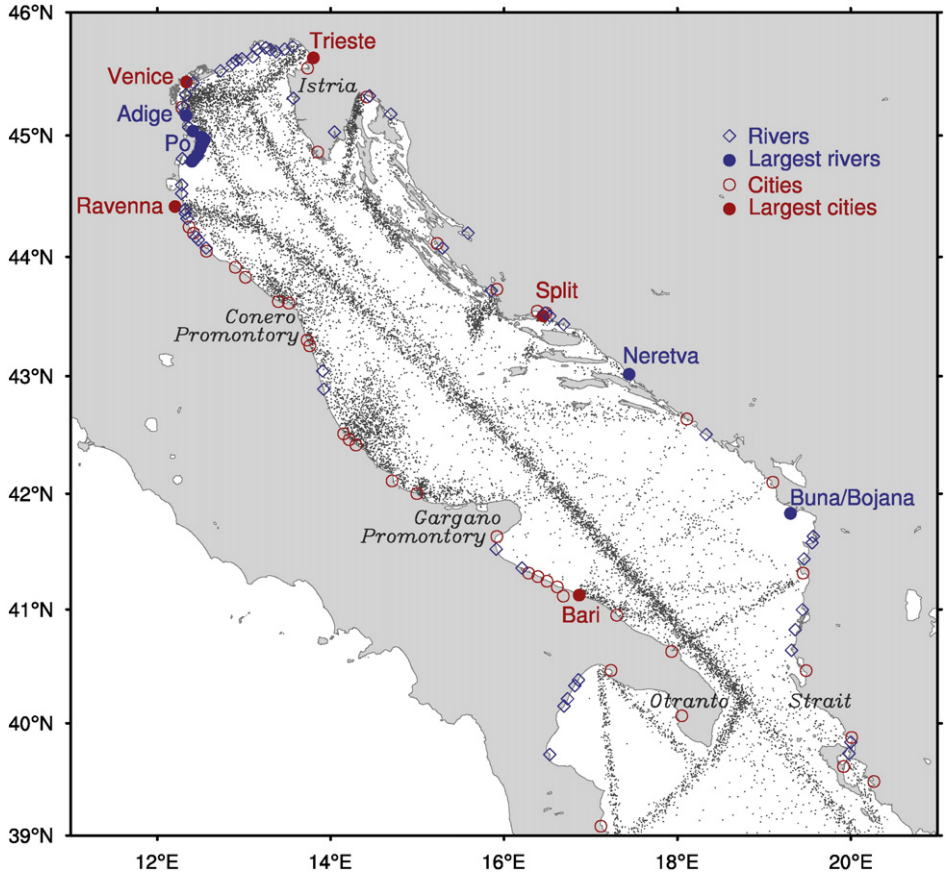

Fig. 1. Spatial distribution of the floating debris inputs into the Adriatic Basin: shipping lanes (gray scatter plot); rivers (open blue diamonds), the largest rivers (closed blue circles); cities (open red circles); and the largest cities (closed red circles).

their contributions to plastics entering the Adriatic Basin through the Otranto Strait. Total river-born plastic input of 4000 ton year $^{-1}$ is distributed to be proportional to the average annual rivers' runoffs. We apply annual averaging in order to be consistent with the annually averaged data on urban population and shipping lanes described below.

Urban population data are taken from a database implemented by Brinkhoff (2010). The 46 largest cities located inside a 10 km coastal belt, which contained more than 20,000 inhabitants in 2010, are considered. Three cities situated on the north Ionian Sea coast are included due to their possible contribution to the floating debris flux through the Otranto Strait. Total coastal urban population input of 4000 ton year $^{-1}$ is distributed to be proportional to the number of each city's inhabitants.

To distribute the total plastic input of 2000 ton year $^{-1}$ along shipping lanes, we extract 60 of the most congested lanes from an annually averaged traffic density map provided by Automatic Identification System (AIS, 2015). Each lane is described by six parameters: the geographical coordinates of the two end-points (longitudes and latitudes), the average traffic intensity, and the width. Applying spatial randomization to these parameters, the possible locations of the marine inputs are generated (Liubartseva et al., 2015). The combined distribution of the inputs described above is presented in Fig. 1. The intensities of the top 10 marine litter inputs into the Adriatic Sea are listed in Table 2. As shown in Table 2, 20% of the total input comes from the shipping lanes, followed by the Po River (13.5%). Bari is a greatest contributor (3.5%) among cities. In general, seven main sources are responsible for more than 50% of total marine litter input, namely shipping lanes (20%), the Po River (13.5%), the Buna/Bojana River (5.8%), Bari (3.5%), Venice (2.9%), the Neretva River (2.8%), and the city of Trieste (2.3%).

In should be noted that we keep all the inputs to be constant from year to year assuming that they do not change substantially over 2009–2015. Due to a lack of information, we also do not apply any seasonality to the inputs.

Table 2
Top 10 marine litter inputs into the Adriatic Basin.

	Input	Intensity (ton year $^{-1}$)	% of total inputs
1	Shipping lanes	2000	20.0
2	Po River	1349	13.5
3	Buna/Bojana River	575	5.8
4	Bari	351	3.5
5	Venice	291	2.9
6	Neretva River	283	2.8
7	Trieste	229	2.3
8	Split	198	2.0
9	Adige River	191	1.9
10	Ravenna	183	1.8
	Other rivers (58) and cities (41)	4350	43.5

2.2. Lagrangian model: MEDSLIK-II

Similar to the majority of Lagrangian models (Fernandes et al., 2013; Zodiatis et al., 2012), the oil spill model code MEDSLIK-II (De Dominicis et al., 2013a,b) is applicable to the case of surface passive tracers that could simulate the behavior of floating plastic debris at a first approximation. In MEDSLIK-II (http://medslikii.bo.ingv.it), each Lagrangian particle moves due to currents, winds, and waves, and follows a

trajectory calculated using advective and diffusive displacements:

$$dx(t) = U(x,y,t)dt + dx'(t)$$
$$dy(t) = V(x,y,t)dt + dy'(t), \quad (1)$$

where $dx'(t)$, $dy'(t)$ are the random walk displacements due to horizontal turbulent diffusion. Two components of the flow velocity, $\mathbf{U} = (U,V)$ are provided by the currents from the external basin-scale or regional oceanographic model. In addition, a Stokes drift-equivalent correction term is taken to be simply proportional to the wind components multiplied by 0.01, in accordance with the work of Kubota (1994).

If a particle arrives on the coast, the model is able to simulate the adsorption of particles into the coastal environment, taking into account a probability that particles may be washed back into the water. As outputs, MEDSLIK-II provides the particle concentrations in two states: at the surface and on the coast. Particle concentrations at the surface and coastline are calculated on a finer grid than the one used in the hydrodynamic model (De Dominicis et al., 2013a); in this work we used a resolution of 150 m. MEDSLIK-II simulates particle concentration on the coast by using a GSHHG coastline (NOAA National Geophysical Data Center, 2014) discretized into segments with a resolution appropriate for each segment, which varies from a few meters to 100 m for an almost straight coastal segment. The Lagrangian time step is taken to be 30 min in MEDSLIK-II.

2.3. Meteo-oceanographic data

As detailed above, MEDSLIK-II requires the input of data about atmospheric winds and sea currents. The atmospheric wind data are provided by the European Centre for Medium-Range Weather Forecasts (ECMWF) analyses, 0.25° horizontal and 6-h temporal resolutions. The ocean current data are provided by daily simulation fields produced by the Adriatic Forecasting System, AFS (http://oceanlab.cmcc.it/afs). AFS uses the POM-based Adriatic regional model as a theoretical background (Guarnieri et al., 2010). The model domain covers the geographical area of 39–45.82° N and 12.2–20.78° E with a horizontal resolution of about 1/45°, which is approximately equal to 2.2 km, on 31 sigma-layers. The bottom topography is obtained from the U.S. Navy 1/60° bathymetric database DBDB1, by bilinear interpolation of the depth data into the model grid. The model is forced by momentum, water, and heat fluxes interactively computed by using model predicted sea surface temperature and the atmospheric ECMWF data at 0.25° horizontal and 6-h temporal resolutions. The river input into the basin has been implemented through river climatology (Raicich, 1994). Precipitation is taken from the global climatological monthly means (Legates and Wilmott, 1990). AFS is nested into the Mediterranean Forecasting System, MFS (Oddo et al., 2009; Pinardi et al., 2003; Tonani et al., 2008). The nesting technique is specified in Zavatarelli and Pinardi (2003), Oddo et al. (2005). Tidal signal is introduced in AFS through the southern lateral open boundary conditions on barotropic velocity.

3. Markov chain model

Following Maximenko et al. (2012) and van Sebille et al. (2012), concentrations of floating particle debris are calculated in two steps:

(1) calculation of the transition matrices by means of the ensemble runs of MEDSLIK-II coupled to the AFS currents and ECMWF wind, and
(2) construction of the Markov chain to simulate the evolution over time of particle concentrations from terrestrial and maritime inputs as identified in Section 2.1.

Although the most logical way is directly aggregating the virtual trajectories (Lebreton et al., 2012; Mansui et al., 2015), we have chosen the Markov chain model to overcome the limitation on the integration time of 10 days imposed by the Lagrangian model MEDSLIK-II.

3.1. Calculation of the transition matrices

In order to compose a model dataset, the suites of 10,000 virtual floating particles are released instantaneously from each cell of the AFS grid (number of grid cells is 27,850 including 3622 coastal cells), and tracked by means of MEDSLIK-II. This multiple release is reset after every 10 days over 12 January 2009–30 April 2015 (230 times), which yields a total of more than 6×10^{10} released particles ($27,850\times230\times10,000$). Particles do not interact with each other; therefore, the combined concentration field is calculated using a linear superposition of concentrations resulting from all the releases over the basin. After that, concentration fields from each multiple release are re-gridded onto the AFS grid and stored on a daily basis.

The integration time for Eq. (1) is chosen to be 10 days for the following reasons. Re-gridding induces the effect of finite-range diffusion with range of the order of the grid cell length (Froyland et al., 2007). Consequently, the integration time should be large enough for advective transport to dominate any discretization-induced diffusive transport. In other words, time of integration should be large enough so that most trajectories leave their initial grid cell. In the calculations reported here, at the characteristic velocity of 2 cm s $^{-1}$ in the Adriatic Sea (Lacorata et al., 2001; Veneziani et al., 2007), particles travel a distance of 17 km for 10 days, which significantly exceeds the grid cell length of 2.2 km. However, the Markov chain approach imposes a limitation caused by within-grid-cell correlation between entry and exit of particle (van Sebille et al., 2011; Maximenko et al., 2012). As a consequence, we have underestimated the advection of floating debris by the weak currents of magnitude less than $\frac{\text{grid cell length}}{\text{integration time}} \sim 0.3$ cm s $^{-1}$.

We use the re-gridded data to calculate the transition matrices according to van Sebille et al. (2012), Froyland (2000), Froyland et al. (2014). First of all, we split the interior and coastal grid cells. By definition, the former are described as the particles floating at the sea surface (*srf*). The latter represents the plastic particles on the coast (*cst*). Hence, four types of transition matrices can be introduced as follows.

Matrices $[\mathbf{P}_{k_0k}^{t_0t}]_{srf\to srf}$ express a chance for a particle to move from its initial position k_0 at the sea surface (*srf*) at time t_0 to the final position k at the sea surface (*srf*) at time t. For simplicity of notation, two spatial indices, i and j, are combined into one spatial index k. The interior matrices $[\mathbf{P}_{k_0k}^{t_0t}]_{srf\to srf}$ describe the transport of particles between interior grid cells in probability terms.

Then, $[\mathbf{P}_{k_0k}^{t_0t}]_{srf\to cst}$ indicate a chance for a particle to move from its initial position at the sea surface (*srf*) to a final position at the coast (*cst*).

Matrices $[\mathbf{P}_{k_0k}^{t_0t}]_{cst\to srf}$ signify a chance to move from the initial position at the coast (*cst*) to the final position at the sea surface (*srf*). In the present work, we assume that all the elements of $[\mathbf{P}_{k_0k}^{t_0t}]_{cst\to srf}$ are equal to zero, and perform this by the removing the particles after 10 days of stagnation in the coastal grid cells. Maximenko et al. (2012) performed the same after 5 days of stagnation. It should be emphasized that this assumption plays a key role because it provides dissipativity of the system due to interaction with the coastline.

To complete the consideration, the unit diagonal matrices $[\mathbf{P}_{k_0k}^{t_0t}]_{cst\to cst}$ that express a chance to move from the initial position at the coast (*cst*) to the final position at the coast (*cst*) can be formally introduced.

Following van Sebille et al. (2012), in an attempt to limit randomness of our Markov chain we have used 230 ten-day transition matrices.

3.2. Plastic particles' release experiment

The transition matrices described above provide a statistical summary of the advective-diffusive flow of the Lagrangian particles by the underlying high-resolution atmospheric and oceanographic fields (Froyland, 2000). Once the transition matrices have been obtained, the evolution

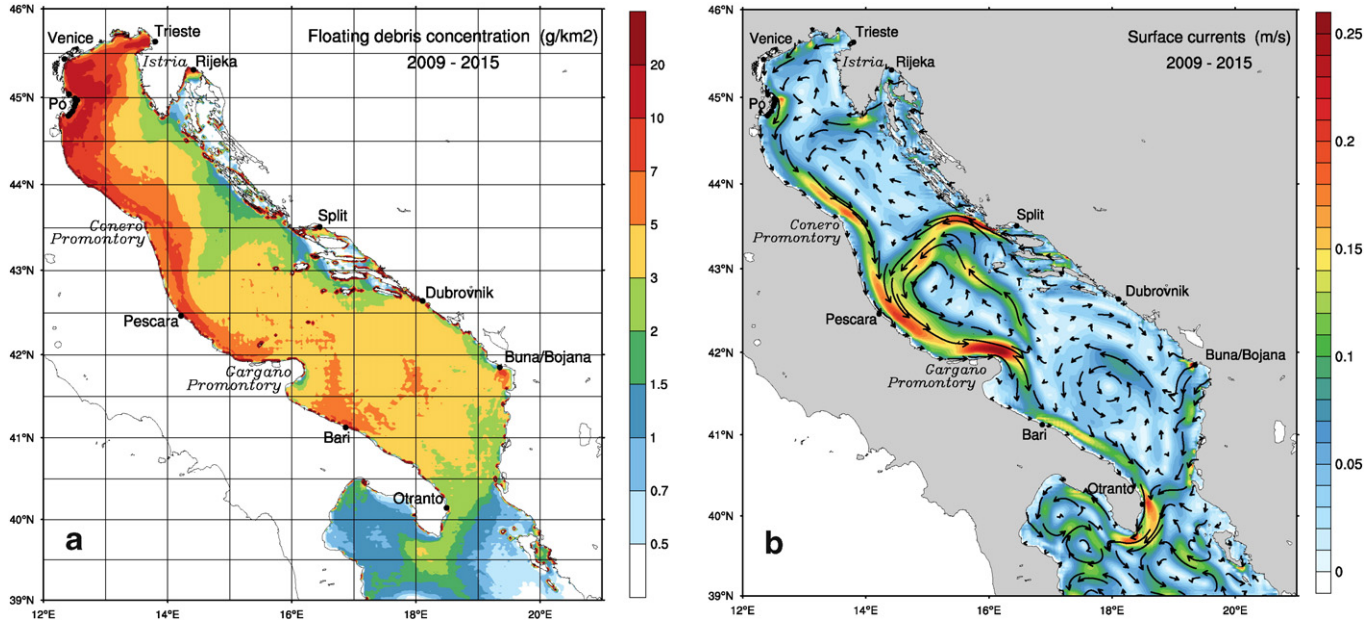

Fig. 2. Averaged 2009–2015 maps (a) of floating debris concentration (g km^{-2}) at the sea surface, and (b) of surface currents (m s^{-1}).

of the particle concentration at the sea surface grid cells $\mathbf{c}_{srf}^{kt_{n+1}}$ and in the coastal grid cells $\mathbf{c}_{cst}^{kt_{n+1}}$ from any source can be iteratively calculated as follows

$$\mathbf{c}_{srf}^{kt_{n+1}} = \mathbf{c}_{srf}^{k_0 t_n} \times \left[\mathbf{P}_{k_0 k}^{t_n t_{n+1}}\right]_{srf \to srf} \tag{2}$$

$$\mathbf{c}_{cst}^{kt_{n+1}} = \mathbf{c}_{cst}^{kt_n} + \mathbf{c}_{srf}^{k_0 t_n} \times \left[\mathbf{P}_{k_0 k}^{t_n t_{n+1}}\right]_{srf \to cst}. \tag{3}$$

Eq. (3) represents accumulation of particles in the coastal cells. In order to meet practical needs, we calculate fluxes of plastic debris onto the coastline segments:

$$\mathbf{f}_{cst}^{k} = \frac{s_{cst}^{k}}{l_{cst}^{k}} \left[\frac{\mathbf{c}_{cst}^{kt_2} - \mathbf{c}_{cst}^{kt_1}}{t_2 - t_1}\right], \tag{4}$$

where s_{cst}^{k} is the area of the coastal cell; l_{cst}^{k} is the length of the coastal segment; and $\mathbf{c}_{cst}^{kt_1}$ and $\mathbf{c}_{cst}^{kt_2}$ are plastic concentrations at time t_1 and t_2, respectively.

Quantification of the fluxes (Eq. (4)) allows us to estimate plastic deposits on the coastline. For example, if we know the residence time of marine plastics on the beach τ (Kataoka and Hinata, 2015), the deposits of plastic particles on coastline can be calculated as

$$\mathbf{d}_{cst}^{k} = \mathbf{f}_{cst}^{k} \tau. \tag{5}$$

If we define a cleanup period of $t_{cleanup}$ as the time period between regular cleanups, mean deposit of plastics can be estimated as

$$\mathbf{d}_{cst\ cleanup}^{k} = \mathbf{f}_{cst}^{k} t_{cleanup}. \tag{6}$$

Deposit values calculated by Eqs. (5) and (6) can be used to plan cleanup activities.

To calculate correctly the particle concentration in the Otranto Strait, the southern boundary of the domain is expanded to 39° N, which is a southern boundary of AFS. At this boundary, zero inflow of particles is imposed. Particles that outflow are removed from the domain as if the 39° N boundary would serve as an artificial coastline. During the time period of 2009–2015, percentage of outflowing particles does not exceed 0.7% of the total particles in the domain. However, due to influence of the southern lateral open boundary conditions we have underestimated the floating debris concentrations and the coastal fluxes in the southern part of the domain, particularly in the Northern Ionian Sea.

After the gridding of each marine litter input specified in Section 2.1 onto the AFS grid, and the spreading over the four closest grid cells, the instantaneous pulses of particles are initialized periodically from each input. As previously detailed in van Sebille et al. (2012), these pulse-like releases tend to provide clearer patterns of particles' behaviors over time. In the present calculations, each pulse is activated on a synoptic time scale of 10 days over the period from January 2009 to April 2015, including a spin-up period that will be justified in Section 4.1.

In the framework of the methodology described above, we interpret virtual floating particles as plastic marine debris. It should be noted that, some important natural processes have been neglected, including plastic that sinks due to a loss of buoyancy caused by biofouling and adherence of inorganic particles (Muthukumar et al., 2011; Woodall et al., 2014). Additionally, breaking into microplastics and ingestion by biota (Andrady, 2011; Cole et al., 2011) are not considered. All of these issues need to be better understood and quantified, and should be taken into account in further modeling.

4. Results and discussion

4.1. Half-life time of particles as a measure of dissipativity of the basin

Half-life time of floating particles is an important transport characteristic of the basin that stems from the basin geometry and dynamics. We estimate this value by means of a long-time integration of Eqs. (2) and (3). The mean particle half-life, i.e., the time after release at which 50% of the particles still remain at the sea surface, is found to be approximately 43.7 days, which is in good agreement with the drifter mean half-life of 40 days observed by Poulain (2001) in the Adriatic Sea. According to this value, the Adriatic Sea, as a land-locked basin, is defined as a highly dissipative system with respect to floating plastics, in contrast to the global ocean, where the half-life time of particles equals 19 years (Maximenko et al., 2012).

It should be noted that a 6-year integration of Eqs. (2) and (3) does not reveal any so-called garbage patches in the Adriatic Sea, which is identical to the conclusion drawn by Mansui et al. (2015) for the Mediterranean Sea. However, substantial accumulation of plastics on the coastline is obtained, which is logically implied from Eqs. (2) and (3) as a consequence of the mass conservation law. Thus, in the present work, shoreline is, by construction, the main sink of plastic debris. In reality, the sink is mainly partitioned between the shoreline and seafloor (Galgani et al., 2000), but we could not calculate in which proportion because loss of the plastic buoyancy is still unknown.

To compute correctly the floating debris concentration, a spin-up period of 90 days, which exceeds a double half-life time, is taken into account. This allows avoidance of any depletion in concentration fields at the beginning of calculations.

Table 3
Worldwide measurement of concentration of plastic debris floating at the sea surface in mass concentration units.

Domain	Concentration (g km $^{-2}$)	Reference
Global Ocean	1–10,000	Eriksen et al. (2014)
North Pacific Garbage Patch	300–3500	Wong et al. (1974)
	46–1210	Day and Shaw (1987)
	64–30169	Moore et al. (2001)
	3600	Yamashita and Tanimura (2007)
	70.96 (mean)	Eriksen et al. (2014)
North Atlantic Garbage Patch	290 (mean)	Carpenter and Smith (1972)
South China Sea	16.7 (mean)	Zhou et al. (2011)
Mediterranean Sea	22–1934, 423 (mean)	Cozar et al. (2015)

4.2. Concentration of plastic debris floating at the sea surface and its flux onto coastline

After integration of Eqs. (2) and (3), daily averaged distributions of plastic debris concentration are obtained for both the interior and coastal cells. A short animation of the floating debris drift over 2013–2015 is presented to show spatial–temporal variability of the concentration fields on a daily scale (http://plastics.cmcc.it/files/DFG_suppl.mov). Fluxes of plastics onto the coastline are calculated based on concentrations in the coastal cells by means of Eq. (4).

Starting our analysis from the averaged 2009–2015 map of debris concentration at the sea surface (Fig. 2), we compare our results with available field observations (Table 3). Unfortunately, the majority of the observations count debris items per square kilometer, which does not allow a direct comparison with our model results. Taking into account the differences in the inputs and dissipativity among various domains with respect to floating debris, it can be concluded that the calculated concentrations that vary in the range of 0–60 g km^{-2} (Fig. 2a) are in reasonable quantitative agreement with the field observations, at least as far as the order of magnitude is concerned.

Turning our focus to spatial variability of the concentration field (Fig. 2a), we note that areas of the highest concentrations of plastics (>10 g km^{-2}) are represented by an elongated band shifted to the Italian coastline narrowing from northwest to southeast. In the northern Adriatic, this area almost covers the waters between the Po Delta and Gulf of Trieste. The band has discontinuities at the Gargano Promontory, and then recovers in the waters in front of Bari.

The floating debris concentration tends to correspond to the spatial distribution of the plastic debris inputs (Fig. 1); however, some connections with the known patterns of the general circulation (Artegiani et al., 1997; Oddo et al., 2005; Zavatarelli and Pinardi, 2003) are also clearly visible (Fig. 2b). The shape of the band follows the climatological shape of the intense current jet stretched against the western Adriatic coast, the so-called Western Adriatic Coastal Current. Along the transversal line off Bari, the distribution reveals a penetration of plastics toward the Adriatic interior caused by the so-called South Adriatic gyre (Zavatarelli and Pinardi, 2003). Apart from the elongated band, the distribution reveals elevated concentrations in a semi-closed area slightly south of the Buna/Bojana Mouth and near Rijeka. Although the former is connected with a high local input from the Buna/Bojana River (Table 2), and the latter is caused by the mutual inputs from Rijeka and the Rjecina River (Fig. 1), both areas exhibit very steady water stagnation (Fig. 2b). Additionally, a great number of local high-concentration lenses are obtained near the coast, particularly along the rugged eastern shoreline. Their typical sizes range from a few kilometers to several tens of kilometers. We also associate these features with the areas of relatively weak circulation.

Seasonal averaging the plastic debris concentration is carried out according to the regional climatological seasonality defined by Artegiani et al. (1997) as follows: winter is January–April, spring is May–June, summer is July–October, and autumn is November–December. The seasonally averaged concentrations (Fig. 3a–d) show some general points of agreement among each other and with the total average map (Fig. 2a) described above: the elongated band and local coastal lenses. At the same time, substantial variability is revealed, which is driven by seasonally varying meteo-oceanographic conditions. As Fig. 3e–h shows, boundary currents and jets representing the Adriatic general circulation tend to vary in strength in different seasons.

In winter (Fig. 3a), a lateral extension of the area of elevated concentrations is found, particularly in the middle and southern Adriatic. The reasons this feature appears are rather complex (Fig. 3e), namely: (1) interconnection of the South Adriatic gyre with a notable inflow of water from the Otranto Strait, (2) reinforcement of the Middle Adriatic cyclonic gyre by the Eastern Southern Adriatic Current which is well-developed in winter, and (3) a relative weakness of the outflow through the Otranto Strait such that it is unable to efficiently ventilate the middle and southern Adriatic.

In spring (Fig. 3b), plastic debris tends to be trapped in the northern Adriatic at concentrations of more than 20 g km^{-2} due to a distinct cyclonic circulation deflecting the plastics from the Po Delta and Venice Lagoon toward the Gulf of Trieste and vice versa (Fig. 3f). The area of highest concentrations spreads up to the Istrian Peninsula. Additionally, patchy traces of elevated concentrations are found near Bari and in the southeastern sector of the basin where the South Adriatic gyre is located (Fig. 3f).

In summer (Fig. 3c), the band of elevated concentrations tends to shrink toward the Italian coastline. In the middle Adriatic, longitudinal gradients of plastic concentrations become sharper. Due to a well-developed outflow from the Otranto Strait (Fig. 3g), the southern Adriatic is efficiently ventilated, which leads to a cleansing of the plastics from the southern and middle parts of the basin.

In autumn (Fig. 3d), the belt shows a longitudinal widening in the northern Adriatic. It detaches from the coastline at Conero Promontory and comes back near Pescara. Dispersed patches in floating debris concentrations are visible slightly north of Gargano Promontory, where the very strong Middle Adriatic gyre is located (Fig. 3h). In the southeastern part of the basin, an obvious increase in concentrations up to 7–10 g km^{-2} is found, which can be identified as a notable peculiarity of the season. This feature can be caused by a tight connection between the eastern side of the South Adriatic gyre and a well-defined inflow of water through the Otranto Strait (Fig. 3h).

Fig. 3. Seasonally averaged maps of plastic concentration (g km^{-2}) at the sea surface (left panel) and surface currents (m s^{-1}) (right panel): (a), (e) winter; (b), (f) spring; (c), (g) summer; and (d), (h) autumn.

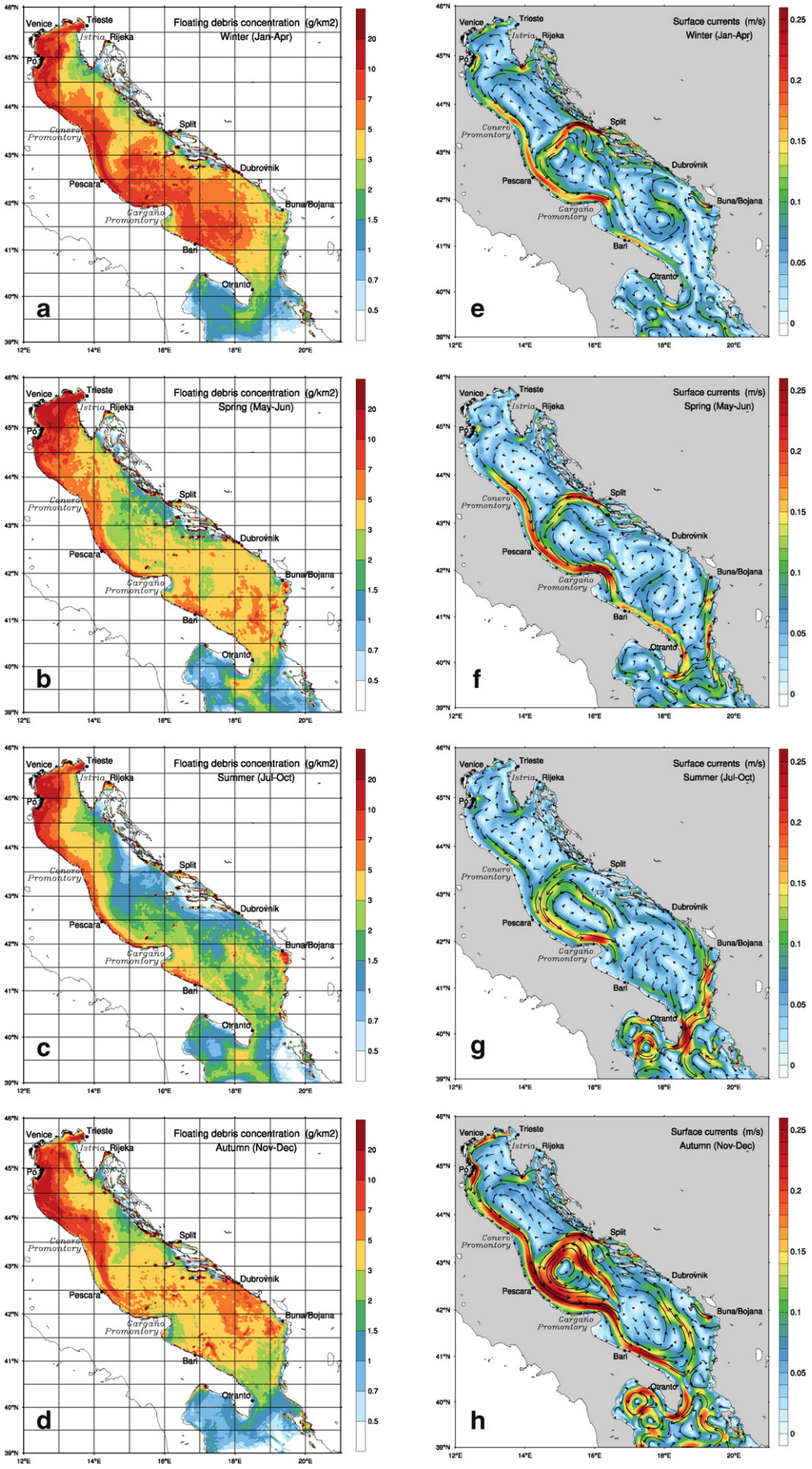
Floating debris concentration (g/km2)
Winter (Jan-Apr)
Surface currents (m/s)
Winter (Jan-Apr)
Floating debris concentration (g/km2)
Spring (May-Jun)
Surface currents (m/s)
Spring (May-Jun)
Floating debris concentration (g/km2)
Summer (Jul-Oct)
Surface currents (m/s)
Summer (Jul-Oct)
Floating debris concentration (g/km2)
Autumn (Nov-Dec)
Surface currents (m/s)
Autumn (Nov-Dec)
Venice
Trieste
Istria
Rijeka
Po
Split
Conero Promontory
Dubrovnik
Pescara
Gargano Promontory
Buna/Bojana
Bari
Otranto
a
b
c
d
e
f
g
h
12°E
14°E
16°E
18°E
20°E
39°N
40°N
41°N
42°N
43°N
44°N
45°N
46°N
20
10
7
5
3
2
1.5
1
0.7
0.5
0.25
0.2
0.15
0.1
0.05
0

Plastic debris fluxes onto coastline are calculated for the 54 selected coastal segments over the 6-year interval (t_1 = 1 May 2009, t_2 = 30 April 2015 in Eq. (4), and are plotted in Fig. 4. Fig. 4a shows a pronounced asymmetry in plastic debris fluxes between the eastern and western coastlines of the Adriatic Basin (Fig. 4b): the eastern part (from Igoumenitsa to the Marano Lagoon) tends to get less plastic debris than the western one (from the Marano Lagoon to Crotone). The distinctive "hot spots" are found in the Po Delta (70.1 kg(km day)$^{-1}$); Venice (35.8 kg(km day)$^{-1}$); Chioggia (32.6 kg(km day)$^{-1}$) and in the Reno Mouth (25.3 kg(km day)$^{-1}$). Bari receives a plastic debris flux of 24.2 kg(km day)$^{-1}$), followed by the western coastline by Marina di Ravenna (21.7 kg(km day)$^{-1}$), Ancona (16.9 kg(km day)$^{-1}$), and Pesaro (15.4 kg(km day)$^{-1}$). Pula, situated at the southern tip of the Istria Peninsula, demonstrates the highest flux (24.9 kg(km day)$^{-1}$) of the eastern coastline of the Adriatic Basin, followed by the Island of Mljet (18.8 kg(km day)$^{-1}$) and Split (15.7 kg(km day)$^{-1}$).

Applying the residence time of marine plastics on the beach of τ = 209 days (Kataoka and Hinata, 2015), we obtain (Eq. (5)) more than 14 ton km^{-1} of plastic debris deposit in the Po Delta, if no cleanup is conducted. If we apply a regular cleanup once every 10 days, we get

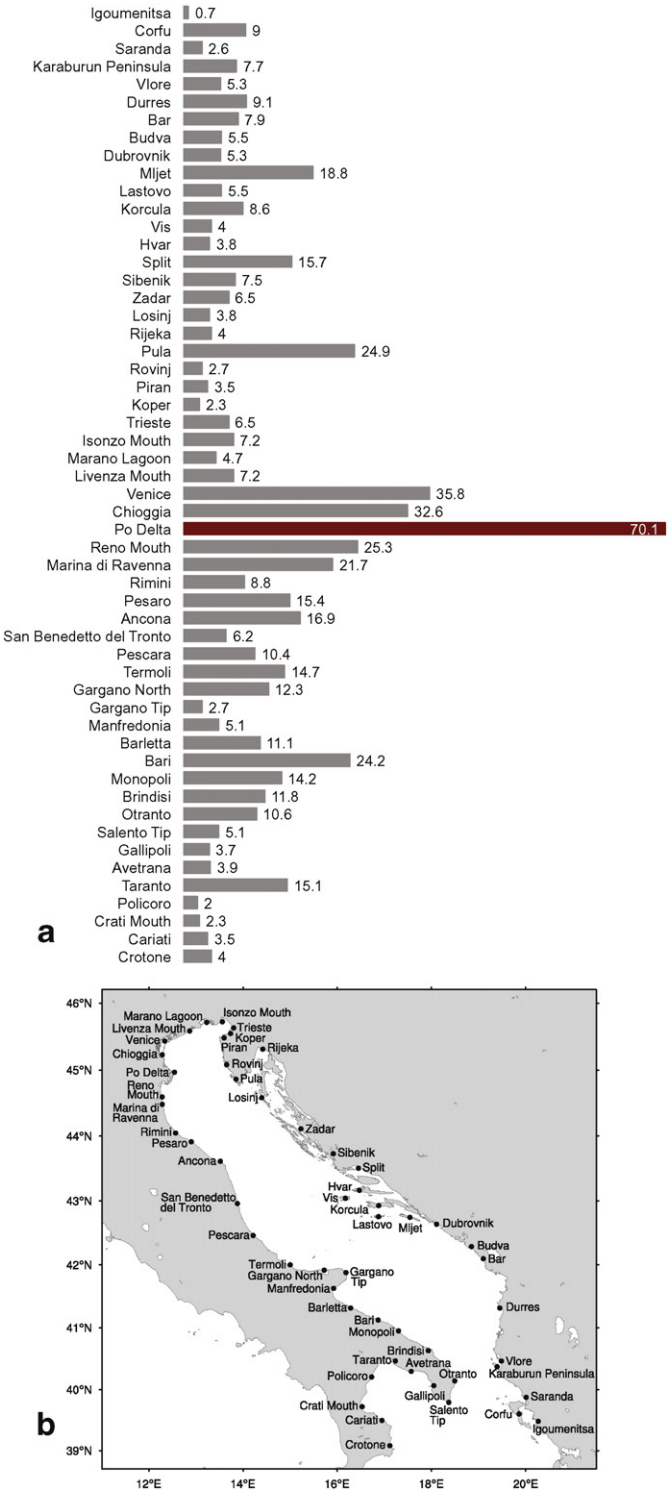

Fig. 4. (a) Plastic debris fluxes (kg(km day)$^{-1}$) onto the Adriatic coastline (2009–2015). The maximum flux in the Po Delta is highlighted in red. (b) Locations of the coastal segments named after the nearby geographic objects.

Table 4
Seasonal variability of floating debris fluxes kg(km day)$^{-1}$ onto the Adriatic coastline.

Coastal Segment	Floating debris flux onto coastal segment (kg(km day)$^{-1}$)			
	Winter (Jan–Apr)	Spring (May–Jun)	Summer (Jul–Oct)	Autumn (Nov–Dec)
Igoumenitsa	0.4	1.0	0.9	0.3
Corfu	9.2	7.7	8.6	10.8
Saranda	2.3	2.9	3.1	2.1
Karaburun Peninsula	6.1	9.1	9.1	7.0
Vlorë	3.2	9.9	6.7	2.3
Durrës	5.3	14.8	13.3	2.2
Bar	6.9	10.6	6.7	9.6
Budva	6.5	6.8	1.9	9.7
Dubrovnik	6.3	6.9	2.3	7.6
Mljet	22.9	19.9	12.4	22.7
Lastovo	7.8	4.9	1.8	8.8
Korcula	10.8	6.9	5.5	12.1
Vis	5.9	3.0	1.7	5.9
Hvar	4.1	3.5	2.9	5.0
Split	14.8	15.5	16.5	15.8
Šibenik	8.4	7.3	6.2	8.5
Zadar	6.8	7.4	6.2	5.5
Lošinj	3.3	5.3	3.8	3.4
Rijeka	3.3	4.8	4.1	4.7
Pula	23.2	26.7	23.3	29.5
Rovinj	1.5	6.2	2.8	1.5
Piran	1.5	2.1	3.4	0.9
Koper	1.0	4.0	3.5	0.5
Trieste	5.7	10.5	6.4	4.4
Isonzo Mouth	8.1	9.2	5.7	6.7
Marano Lagoon	3.8	8.1	4.8	2.6
Livenza Mouth	5.3	13.1	6.5	6.7
Venice	28.5	53.2	41.7	20.9
Chioggia	40.7	21.9	33.7	25.0
Po Delta	**66.2**	**63.7**	**78.5**	**67.1**
Reno Mouth	25.3	20.0	31.0	19.1
Marina di Ravenna	16.8	19.9	28.9	18.9
Rimini	7.1	6.7	11.6	8.7
Pesaro	17.4	11.3	15.4	15.7
Ancona	21.3	12.8	13.5	19.0
San Benedetto del Tronto	6.4	6.7	6.9	3.6
Pescara	9.4	15.0	11.3	6.1
Termoli	17.0	18.6	13.9	8.0
North Gargano	16.1	12.6	9.8	9.5
Gargano Tip	3.8	1.6	1.9	3.0
Manfredonia	4.3	5.3	6.3	4.2
Barletta	8.6	12.3	15.5	5.5
Bari	23.9	29.9	26.6	14.1
Monopoli	14.8	21.6	12.9	8.0
Brindisi	13.3	14.4	11.2	7.5
Otranto	9.1	16.7	12.7	3.1
Salento Tip	4.7	5.4	6.1	3.4
Gallipoli	3.3	4.6	3.6	3.5
Avetrana	4.4	2.5	3.0	6.0
Taranto	15.0	16.3	14.7	14.9
Crati Mouth	1.7	2.3	3.2	1.8
Cariati	1.6	4.1	6.0	1.5
Crotone	1.6	4.7	5.7	2.4

mean deposition of about 700 ton km $^{-1}$ (Eq. (6)) for the period between cleanups.

Although there is considerable similarity between the seasonally averaged 2009–2015 plastic debris fluxes onto coastlines (Table 4) and the flux over the whole 6-year interval of integration (Fig. 4), the temporal variability caused by the meteo-oceanographic conditions is also visible. The Po Delta receives the maximum fluxes of the basin that peak in the summer season (July–October) at up to 78.5 kg(km day)$^{-1}$. Venice and Chioggia demonstrate the elevated fluxes in all the seasons. Fluxes to Venice dominate the fluxes to Chioggia in spring (May–June) and summer (July–October) but fall behind in autumn (November–December), and particularly in winter (January–April). There are coastline segments that receive high and stable fluxes of plastics (in a sequence of winter–spring–summer–autumn), namely, on the eastern coastline: Split (14.8–15.5–16.5–15.8 kg(km day)$^{-1}$) and Pula (23.2–26.7–23.3–29.5 kg(km day)$^{-1}$); on the western coastline: Reno Mouth (25.3–20.0–31.0–19.1 kg(km day)$^{-1}$), Marina di Ravenna (16.8–19.9–28.9–18.9 kg(km day)$^{-1}$), Pesaro (17.4–11.3–15.4–15.7 kg(km day)$^{-1}$), Gargano North (16.1–15.5–9.8–9.5 kg(km day)$^{-1}$). Saranda (2.3–2.9–3.1–2.1 kg(km day)$^{-1}$), Koper (1.0–4.0–3.5–0.5 kg(km day)$^{-1}$), and Gargano Tip (3.8–1.6–1.9–3.0 kg(km day)$^{-1}$) receive permanently low fluxes. In contrast, some locations exhibit seasonal contrasts. For example, the coastline near Durres gets approximately six times more flux (14.8 kg(km day)$^{-1}$) in spring than in autumn (2.2 kg(km day)$^{-1}$). The coastline segment in the vicinity of Bari receive a flux of 29.9 kg(km day)$^{-1}$ in spring in contrast to 14.1 kg(km day)$^{-1}$ in autumn. The Croatian Island of Mljet collects 22.9 kg(km day)$^{-1}$ in winter but 12.4 kg(km day)$^{-1}$ in summer. Hence, a common practice of neglecting cleanups in winter is not suitable for Mljet Island. To sum up, Split exhibits the lowest seasonal max/min ratio of 1.1, while Piran shows the highest seasonal min/max ratio of 10.2.

4.3. Regional approach to modeling the floating debris transport

To study source-receptor interconnections among various subregions in the Adriatic basin, a regional approach was developed. It is aimed at the practical needs of (1) researchers who implement a strategy of plastic litter monitoring at sea; (2) stakeholders involved in coastal cleanup; and (3) policy makers who develop regulations on discharge of garbage in the marine environment. Formally, the methodology is based on forward-in-time (so called direct problem) and backwards-in-time (so called inverse problem) integration of Eqs. (2) and (3) with respect to a selected set of the subregions of interest.

Fig. 5 shows the division of the Adriatic basin into the 30 selected subregions comprising 26 coastal and four open-sea subregions. In the present work, the division is based on the basin geography and major patterns of the general circulation (Artegiani et al., 1997). Depending on the research interest, it can be also conducted on the basis of coastal geomorphology or the administrative structure, economics, geopolitics, and so forth.

The solution to the direct and inverse problems will be illustrated below in an example of a 13th subregion (44.0–44.7° N 12.0–13.0° E), which is a part of the Italian administrative region Emilia Romagna (Fig. 6). We chose this subregion because recent field observations (Mazziotti et al., 2015) reveal the elevated concentration of plastics there which stem from the direct influence of the Po inputs.

4.3.1. Direct problem

As shown in Fig. 6, the inputs from a 13th subregion of Emilia Romagna consist of the plastic debris fluxes from the shipping lanes; the rivers of Marecchia with a mean value of 104 ton year $^{-1}$, Reno (43 ton year $^{-1}$), Lamone (11 ton year $^{-1}$), Uniti (11 ton year $^{-1}$), Savio (11 ton year $^{-1}$), Bevano (5 ton year $^{-1}$), Rubicone (5 ton year $^{-1}$), Uso (5 ton year $^{-1}$); and the cities of Ravenna (183 ton year $^{-1}$), Rimini (163 ton year $^{-1}$), Cervia (32 ton year $^{-1}$), Cesenatico (29 ton year $^{-1}$).

Forward-in-time integration of Eqs. (2) and (3) is carried out to calculate the relative contribution of the floating debris inputs from the 13th subregion to each subregion of the Adriatic basin. As Table 5 indicates, the main receptor (36.3%) coincides with the main source: Emilia Romagna subregion. Together with the second receptor of North Marche (19.8%), they collect more than half of the floating debris from Emilia Romagna. The rest is redistributed at sea mainly following the Western Adriatic Coastal Current that tends to dominate along the

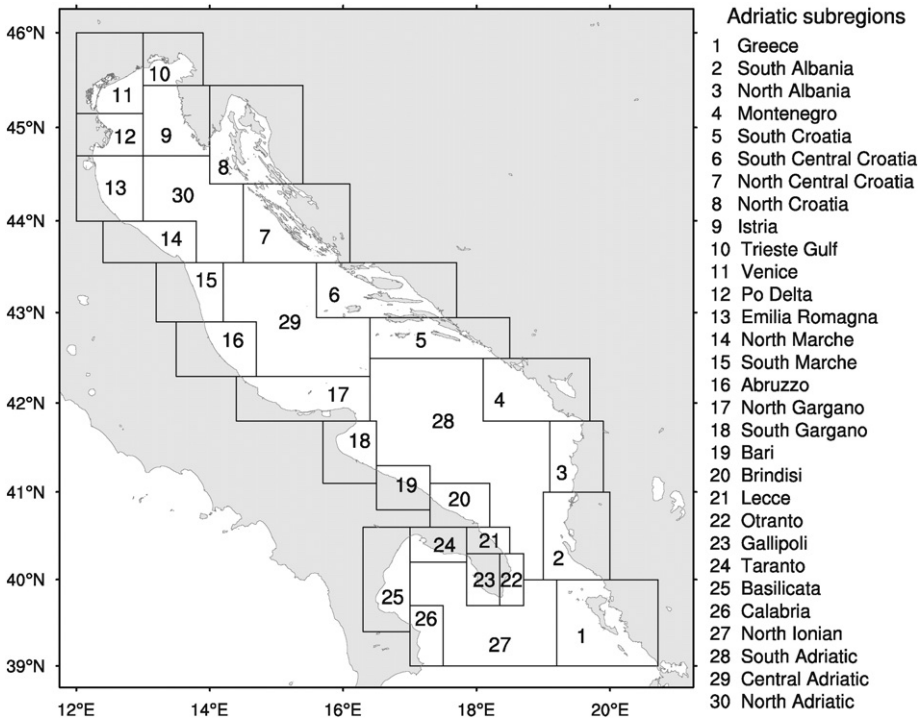

Fig. 5. Division of the Adriatic Basin into the subregions named after nearby geographic objects.

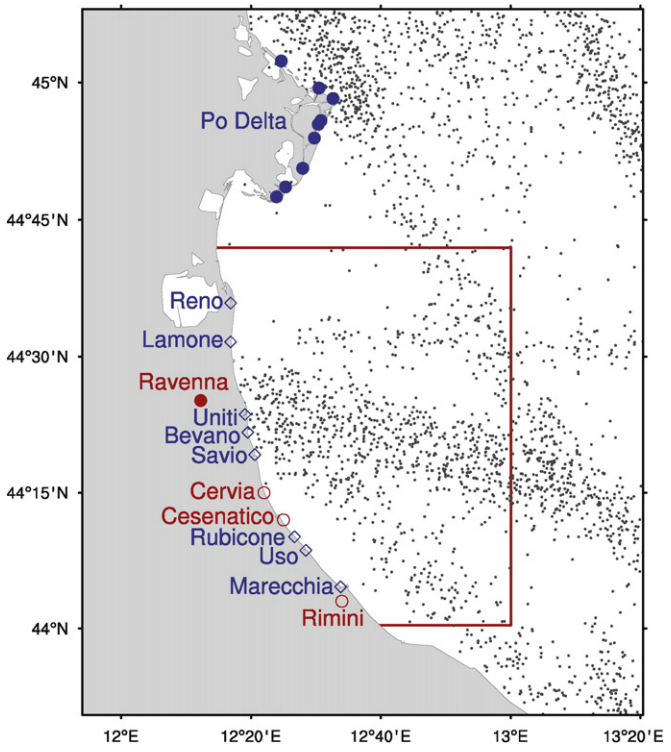

Fig. 6. The enlarged 13th subregion and the inputs of floating debris labeled as in Fig. 1: shipping lanes (gray scatter plot); rivers (open blue diamonds), the largest rivers (closed blue circles); cities (open red circles); and the largest cities (closed red circles).

western coastline of the basin. Due to across-basin transport some minor receptors are found on the eastern coastline of the basin, namely 3.1% in North Croatia, 2.5% in North Central Croatia, 2.0% in South Central Croatia, and 1.9% in South Croatia. In total, the eastern coastline receives more than 9% of the floating plastic debris from Emilia Romagna.

4.3.2. Inverse problem

To identify the relative contribution of the floating debris inputs from each subregion to a 13th subregion, the backwards-in-time integration of Eqs. (2) and (3) is conducted. As Table 6 indicates, the main polluter of Emilia Romagna with respect to plastic debris is the subregion of the Po Delta which accounts for 46.0% of contamination. This fraction even exceeds Emilia Romagna's own contribution of 35.0%. Others, including Venice, the Trieste Gulf, Istria, and items 6–10 listed in Table 6 are in total responsible for only 18.0% of the plastics.

Additionally, we calculate the relative contributions from each floating debris input depicted in Fig. 1. Unsurprisingly, the 13th subregion is mostly influenced by the Po River (Table 7), which together with the city of Ravenna is responsible for more than 50% of the plastic accumulated on the coastline of Emilia Romagna.

Table 6
Top 10 source-subregions contributing the floating debris (%) to the 13th subregion of Emilia Romagna (2009–2015).

	Subregion-source (number)	% of all subregion-sources
1	Po Delta (12)	46.0
2	Emilia Romagna (13)	35.0
3	Venice (11)	6.8
4	Trieste Gulf (10)	6.4
5	Istria (9)	2.2
6	North Marche (14)	1.3
7	North Adriatic (30)	0.5
8	Montenegro (4)	0.3
9	Abruzzo (16)	0.3
10	South Albania (2)	0.2

4.3.3. Impact matrices

The direct problem described above can be generalized to quantify the source–receptor relationships among all the Adriatic subregions. To present the results we have introduced a direct impact matrix (Fig. 7). The rows of the matrix represent the subregions that are considered sources of the floating debris. The columns indicate the subregions that serve as the receptors of plastics. The matrix elements are colored according to their relative contributions in percent. We have introduced the 31st row and column to take into consideration the floating debris that leaves the domain through the open 39° N boundary. Then, a sum of all the elements in the row equals 100%. For example, the floating debris from the 3rd subregion of North Albania is distributed as follows: approximately 30–50% remains in North Albania; 20–30% goes to Montenegro and South Croatia; 5–10% to South Albania; 1–5% to North Gargano, Bari, Brindisi, Lecce, Otranto, Gallipoli, and out of the domain. Other subregions receive less than 1%.

As indicated in Fig. 7, the maximum values tend to be located on the main diagonal of the impact matrix. This indicates that a major part of floating debris tends to beach onto the coastline of its own subregion-source. However, there are some exceptions, namely South Marche and Abruzzo send a majority of their plastics to North Gargano. Keeping in mind that these features are obtained on the long-term integration (2009–2015), we can conclude that such a local self-cleansing is provided by a stable, long-term Western Adriatic Coastal Current. The appearance of the significant matrix elements that are far from the main diagonal of the matrix provide evidence about the across-basin exchange. Such a process is revealed for the eastern subregions of Montenegro and South Croatia, and for the western subregions of North Gargano, Bari, Brindisi, and Lecce. The inputs from the open-sea subregions constitute only off-shore contributions from the shipping lanes. As shown in Fig. 7 30–50% of plastics from the ships in the North and Central Adriatic go to North Gargano, while 20–30% from the ships in the South Adriatic go to South Croatia. The plastics from

Table 5
Top 10 subregion-receptors receiving the floating debris (%) from the 13th subregion source of Emilia Romagna (2009–2015).

	Subregion-receptor (number)	% of all Subregion-receptors
1	Emilia Romagna (13)	36.3
2	North Marche (14)	19.8
3	North Gargano (17)	12.0
4	South Marche (15)	3.7
5	North Croatia (8)	3.1
6	Abruzzo (16)	2.9
7	Bari (19)	2.6
8	North Central Croatia (7)	2.5
9	South Central Croatia (6)	2.0
10	South Croatia (5)	1.9

Table 7
Top 10 inputs contributing the floating debris (%) to the 13th subregion-receptor of Emilia Romagna (2009–2015).

	Input	% of all inputs
1	Po River	39.1
2	Ravenna	14.0
3	Shipping lanes	10.8
4	Rimini	6.8
5	Reno River	3.7
6	Adige River	3.0
7	Trieste	2.8
8	Cervia	2.1
9	Cesenatico	1.7
10	Brenta River	1.2

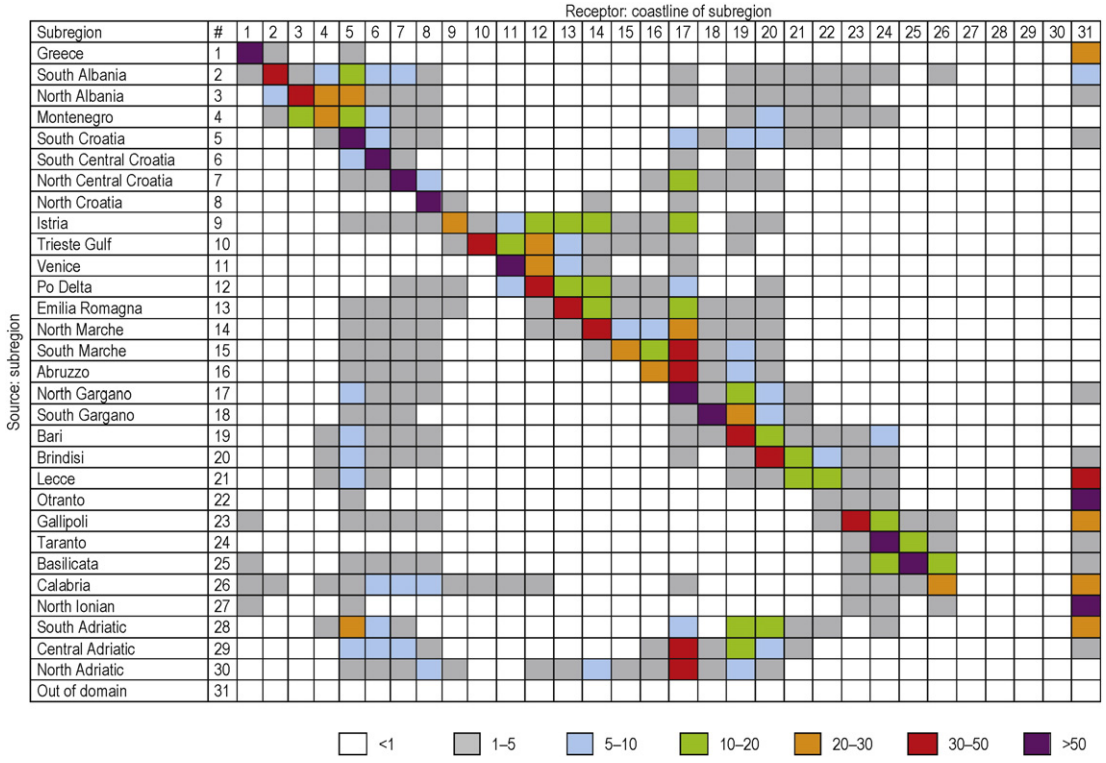

Fig. 7. Direct impact matrix quantified (%) the source–receptor relationships among the subregions in the Adriatic Basin.

the ships in the Ionian Sea tend to leave the domain through the open boundary.

As far as the inverse problem is concerned, the approach also allows the generalization to quantify the receptor-source relationships among all the Adriatic subregions. Thus, an inverse impact matrix can be calculated (Fig. 8). The rows of the matrix represent the subregions whose coastlines receive plastics, that is, receptors, while the columns show the sources. A sum of all elements in the row equals 100%. For example, the coastline of the Bari subregion gets 30–50% from the inputs situated in the home subregion of Bari, 5–10% from North and South Gargano, as well as 5–10% from the shipping lanes located in the South and Central Adriatic.

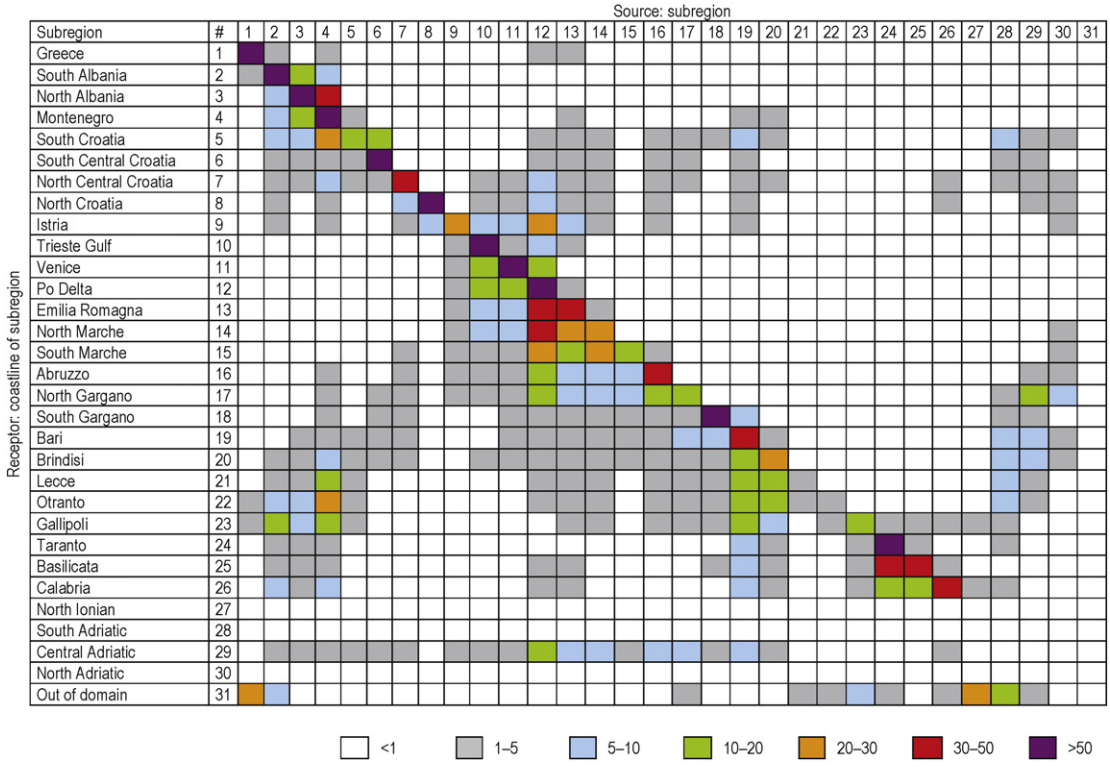

Fig. 8. Inverse impact matrix quantified (%) the receptor–source relationships among the subregions in the Adriatic Basin.

Some subregions collect the floating debris locally, from the nearest neighbors (e.g., North Albania and Venice), while others receive it also from the whole basin including remote sources. For instance, South Croatia collects its own plastic debris (10–20%), and also receives it from the nearest locations: Montenegro (20–30%); South Central Croatia (10–20%); North Albania and the South Adriatic (5–10%); and the Central Adriatic (1–5%). A portion of plastics comes from the opposite locations: Bari (5–10%); and Abruzzo, North Gargano, and South Gargano (1–5%). The rest is received from remote locations including South Albania (5–10%); and the Po Delta, Emilia Romagna, North Marche, Brindisi, and the North Adriatic (1–5%).

5. Conclusions

In the present work, we have shown the first results of modeling the floating debris concentrations at the sea surface and on the coastlines in the Adriatic Basin over 2009–2015. The calculations are based on combining data of terrestrial and maritime plastic litter inputs with the Markov chain model built by means of the Lagrangian model MEDSLIK-II, forced by AFS ocean currents simulations and ECMWF wind analyses. The Markov chain model provides a significant flexibility and computational efficiency in simulating any configuration of the plastic debris inputs, which are very uncertain. Not only does the Markov chain model allow the forward-in-time simulation of plastic concentrations, it also gives an opportunity to perform correctly the backwards-in-time simulation.

The mean particle half-life in the Adriatic is found to be approximately 43.7 days, which allows us to define the Adriatic Sea as a highly dissipative system with respect to floating plastics. By construction, the coastline is the main sink of floating plastic debris. Further consideration of sinking plastic debris is necessary to calculate its distribution on the seabed.

On long-term time-mean scales, floating debris distributions correspond to the spatial distributions of plastic debris inputs (rivers, cities, and shipping lanes), and indicates a tight connection with patterns of the general Adriatic circulation. Thus, the elongated band of elevated concentration at the sea surface (>10 g km^{-2}) follows the climatological shape of the Western Adriatic Coastal Current. Penetration of plastics toward the Adriatic interior opposite Bari is revealed as the evidence of transport by the South Adriatic gyre. Inshore areas and a great number of local lenses with high plastic concentrations seem to be related to coastal areas of weak circulation.

On seasonal time-mean scales, we indicate the winter plastics' expansion into the basin's interior, spring trapping in the northern Adriatic, summer cleansing the middle and southern Adriatic and autumn spreading into the southeastern Adriatic. These seasonal features result mainly from the seasonal variability of the basin scale circulation including Western Adriatic Coastal Current, the South Adriatic gyre, the Middle Adriatic gyre, and the Eastern Southern Adriatic Current.

Distinctive coastal “hot spots” are found: on the Po Delta coastline that receives a plastic flux of 70.1 kg(km day)$^{-1}$; Venice: 35.8 kg(km day)$^{-1}$; Chioggia: 32.6 kg(km day)$^{-1}$; the Reno Mouth: 25.3 kg(km day)$^{-1}$; and Pula, situated at the southern tip of the Istria Peninsula: 24.9 kg(km day)$^{-1}$. As far as seasonality in plastics flux onto coastlines is concerned, the highest seasonal max/min ratio of 10.2 is found in Piran, while Split has the lowest min/max ratio of 1.1.

To meet practical needs the regional approach was developed as follows: (1) the basin is divided into the subregions of interest; (2) the relative contribution of the floating debris inputs from each source-subregion is calculated by solving the direct problem; (3) for each receptor-subregion, the relative contribution from the source-subregion is calculated by solving the inverse problem; and (4) the results are summarized in terms of direct and inverse impact matrices.

Impact matrices built for all the subregions reveal complex source–receptor relationships among the various Adriatic subregions. The example of floating debris that originated from the subregion of Emilia Romagna demonstrates that more than one-third of the plastics are beached on the coastline from which they originate. About 41.0% go southward, to the Italian coastline from North Marche to Bari, while 9.5% is eventually washed ashore in Croatia. Inversely, the coastline of Emilia-Romania receives 46.0% of its beached plastic debris from the Po Delta subregion, 35.0% of its own floating debris, and 15.4% from Venice, the Gulf of Trieste, and Istria combined.

The results obtained can be used to monitor the floating debris, plan cleanups, and make policy-relevant decisions. The methodology developed for the Adriatic Basin can be extended to any other domain, and could be further improved by including consideration of particles sinking, breaking into microplastics, and being ingested by biota. In addition, further investigation of spatial–temporal variability of plastic litter inputs is vital. Furthermore, we believe that in the future higher resolution current data will enhance the Lagrangian representation of floating plastic debris transport.

Acknowledgements

This work has been supported by the DeFishGear (Derelict Fishing Gear Management System in the Adriatic Region (http://www.defishgear.net/) IPA Adriatic strategic project 1° str/00010 implemented with co-funding by the European Union, Instrument for Pre-Accession Assistance (IPA). The authors wish to thank Giogia Verri for developing the Adriatic river database; Francois Galgani for thoughtful advice on boundary conditions for floating debris; Andrej Kržan for initiating a relevant discussion about units for presentation of the model results; and Michela De Dominicis for encouraging appreciation of the first results.

References

AIS, 2015. The database on automatic identification system. http://www.marinetraffic.com (Online accessed: 10-January-2015).
Andrady, A., 2011. Microplastics in the marine environment. Mar. Pollut. Bull. 62, 1596–1605.
Artegiani, A., Bregant, D., Paschini, E., Pinardi, N., Raicich, F., Russo, A., 1997. The Adriatic Sea general circulation. Part II: baroclinic circulation structure. J. Phys. Oceanogr. 27, 1515–1532.
Brinkhoff, T., 2010. The database on city population. http://www.citypopulation.de (Online accessed: 10-January-2015).
Carpenter, E., Smith, K., 1972. Plastic on the Sargasso Sea surface. Science 175, 1240–1241.
Cole, M., Lindeque, P., Halsband, C., Galloway, T., 2011. Microplastics as contaminants in the marine environment: a review. Mar. Pollut. Bull. 62, 2588–2597.
Cozar, A., Sanz-Martin, M., Marti, E., Gonzalez-Gordillo, I., Ubeda, B., Galvez, J., Irigoien, X., Duarte, C., 2015. Plastic accumulation in the Mediterranean Sea. PLoS ONE 10, 1–12, e0121762.
Csanady, G., 1973. Turbulent Diffusion in the Environment. D. Reidel Publishing Company, Dordrecht (NLD).
Day, R., Shaw, D., 1987. Patterns in the abundance of pelagic plastic and tar in the North Pacific Ocean, 1976–1985. Mar. Pollut. Bull. 18, 311–316.
De Dominicis, M., Pinardi, N., Zodiatis, G., Archetti, R., 2013b. MEDSLIK-II, a Lagrangian marine surface oil spill model for short-term forecasting — part 2: numerical simulations and validations. Geosci. Model Dev. 6, 1871–1888.
De Dominicis, M., Pinardi, N., Zodiatis, G., Lardner, R., 2013a. MEDSLIK-II, a Lagrangian marine surface oil spill model for short term forecasting — part 1: theory. Geosci. Model Dev. 6, 1851–1869.
Eriksen, M., Lebreton, L., Carson, H., Thiel, M., Moore, C., Borerro, J., Galgani, F., Ryan, P., Reisser, J., 2014. Plastic pollution in the Worlds Oceans: more than 5 trillion plastic pieces weighing over 250,000 tons afloat at sea. PLoS ONE 9, 1–15, e111913.
Falco, P., Griffa, A., Poulain, P.M., Zambianchi, E., 2000. Transport properties in the Adriatic Sea as deduced from drifter data. J. Phys. Oceanogr. 30, 2055–2071.
Fernandes, R., Neves, R., Viegas, C., 2013. Integration of an oil and inert spill model in a framework for risk management of spills at sea — a case study for the Atlantic area. AMOP 36 Technical Seminar, pp. 326–353.
Froyland, G., 2000. Extracting dynamical behaviour via Markov models. Nonlinear Dynamics and Statistics, pp. 1–33.
Froyland, G., Padberg, K., England, M., Treguier, A., 2007. Detection of coherent oceanic structures via transfer operators. Phys. Rev. Lett. 98 (224503), 1–4.
Froyland, G., Stuart, R., van Sebille, E., 2014. How well-connected is the surface of the global ocean? Chaos 24 (033126), 1–10.
Galgani, F., Leaute, J., Moguedet, P., Souplet, A., Verin, Y., Carpentier, A., Goraguer, H., Latrouite, D., Andral, B., Cadiou, Y., Mahe, J., Poulard, J., Nerisson, P., 2000. Litter on the sea floor along European coasts. Mar. Pollut. Bull. 40, 516–527.
Guarnieri, A., Oddo, P., Pastore, M., Pinardi, N., 2010. The Adriatic Basin Forecasting System new model and system development. Coastal to Global Operational Oceanography: Achievements and Challenges, pp. 184–190.

Isobe, A., Kako, S., Chang, P.H., Matsuno, T., 2009. Two-way particle tracking model for specifying sources of drifting objects: application to the East China Sea shelf. J. Atmos. Ocean. Technol. 26, 1059–1064.
Isobe, A., Kubo, K., Tamura, Y., Kako, S., Nakashima, E., Fujii, N., 2014. Selective transport of microplastics and mesoplastics by drifting in coastal waters. Mar. Pollut. Bull. 89, 324–330.
Jambeck, J., Andrady, A., Geyerand, R., Narayan, R., Perryman, M., Siegler, T., Wilcox, C., Lavender Law, K., 2015. Plastic waste inputs from land into the ocean. Science 347, 768–771.
Kataoka, T., Hinata, H., 2015. Evaluation of beach cleanup effects using linear system analysis. Mar. Pollut. Bull. 91, 73–81.
Kubota, M., 1994. A mechanism of the accumulation of floating marine debris north of Hawaii. J. Phys. Oceanogr. 24, 1059–1064.
Lacorata, G., Aurell, E., Vulpiani, A., 2001. Drifter dispersion in the Adriatic Sea: Lagrangian data and chaotic model. Ann. Geophys. 19, 121–129.
Lebreton, L., Greer, S., Borrero, J., 2012. Numerical modeling of floating debris in the world's oceans. Mar. Pollut. Bull. 64, 653–661.
Legates, D., Wilmott, C., 1990. Mean seasonal and spatial variability in a gauge corrected global precipitation. Int. J. Climatol. 10, 121–127.
Liubartseva, S., De Dominicis, M., Oddo, P., Coppini, G., Pinardi, N., Greggio, N., 2015. Oil spill hazard from dispersal of oil along shipping lanes in the Southern Adriatic and Northern Ionian Seas. Mar. Pollut. Bull. 90, 259–272.
Mansui, J., Molcard, A., Ourmieres, Y., 2015. Modelling the transport and accumulation of floating marine debris in the Mediterranean basin. Mar. Pollut. Bull. 91, 249–257.
Martinez, E., Maamaatuaiahutapu, K., Taillandier, V., 2009. Floating marine debris surface drift: convergence and accumulation toward the South Pacific subtropical gyre. Mar. Pollut. Bull. 58, 1347–1355.
Maximenko, N., Hafner, N., Niiler, J., 2012. Pathways of marine debris derived from trajectories of Lagrangian drifters. Mar. Pollut. Bull. 65, 151–162.
Mazziotti, C., Bertaccini, E., Benzi, M., Martiniand, P., Lera, S., Silvestri, S., Ferrari, C., 2015. Sea surface microplastics distribution on Emilia-Romagna coast (Northwestern Adriatic Sea — Italy): DeFishGear Project preliminary results. Proceedings of the MICRO-2015 Seminar on microplastics issues, p. 27.
Moore, C., Moore, S., Leecaster, M., Weisberg, S., 2001. A comparison of plastic and plankton in the north Pacific central gyre. Mar. Pollut. Bull. 42, 1297–1300.
Muthukumar, T., Aravinthan, A., Lakshmi, K., Venkatesan, R., Vedaprakash, L., Doble, M., 2011. Fouling and stability of polymers and composites in marine environment. Int. Biodeterior. Biodegrad. 62, 276–284.
Neumann, D., Callies, U., Matthies, M., 2014. Marine litter ensemble transport simulations in the southern North Sea. Mar. Pollut. Bull. 86, 219–228.
NOAA National Geophysical Data Center, 2014. Global self-consistent, hierarchical, high-resolution geography database GSHHG. http://www.ngdc.noaa.gov/mgg/shorelines/shorelines.html (Online accessed: 10-January-2015).
Oddo, P., Adani, M., Pinardi, N., Fratianni, C., Tonani, M., Pettenuzzo, D., 2009. A nested Atlantic–Mediterranean Sea general circulation model for operational forecasting. Ocean Sci. Discuss. 6, 1093–1127.
Oddo, P., Pinardi, N., Zavatarelli, M., 2005. A numerical study of the interannual variability of the Adriatic Sea (2000–2002). Sci. Total Environ. 353, 39–56.
Pinardi, N., Allen, I., Demirov, E., De Mey, P., Korres, G., Lascaratos, A., Le Traon, P., Maillard, C., Manzella, G., Tziavos, C., 2003. The Mediterranean ocean forecasting system: first phase of implementation (1998–2001). Ann. Geophys. 21, 3–20.
Pizzigalli, C., Rupolo, V., Lombardi, E., Blanke, B., 2007. Seasonal variability dispersion maps in the Mediterranean Sea obtained from the Mediterranean Forecasting System Eulerian velocity fields. Prog. Oceanogr. 22 (C05012), 1–17.
Poulain, P.M., 2001. Adriatic Sea surface circulation as derived from drifter data between 1990 and 1999. J. Mar. Syst. 29, 3–32.
Poulain, P.M., Hariri, S., 2013. Transit and residence times in the Adriatic Sea surface as derived from drifter data and lagrangian numerical simulations. Ocean Sci. 9, 713–720.
Raicich, F., 1994. Note on flow rates of the Adriatic rivers. Technical Report. CNR Istituto Talassografico Sperimentale, Trieste, pp. 1–8.
van Sebille, E., Beal, L., Johns, W., 2011. Advective time scales of Agulhas leakage to the North Atlantic in surface drifter observations and the 3D OFES model. J. Phys. Oceanogr. 41, 1026–1034.
van Sebille, E., England, M., Froyland, G., 2012. Origin, dynamics and evolution of ocean garbage patches from observed surface drifters. Environ. Res. Lett. 7 (044040), 1–6.
Thompson, R., Moore, C., Vom Saal, F., Swan, S., 2009. Plastics, the environment and human health: current consensus and future trends. Philos. Trans. R. Soc. Lond. Ser. B Biol. Sci. 364, 2153–2166.
Tonani, M., Pinardi, N., Dobricic, S., Pujol, I., Fratianni, C., 2008. A high-resolution free-surface model of the Mediterranean Sea. Ocean Sci. 4, 1–14.
Ursella, L., Poulain, P.M., Signell, R., 2006. Surface drifter derived circulation in the northern and middle Adriatic Sea: response to wind regime and season. J. Geophys. Res. 111 (C03S04), 1–14.
Veneziani, M., Griffa, A., Poulain, P.M., 2007. Historical drifter data and statistical prediction of particle motion: a case study in the central Adriatic Sea. J. Atmos. Ocean. Technol. 24, 235–254.
Verri, G., Pinardi, N., Oddo, P., Ciliberti, S., Coppini, G., 2014. The influence of the river inflow on the circulation and dynamics of the Adriatic and Northern Ionian Sea. EGU General Assembly 2014 (pp. EGU2014, 16855).
Wong, C., Green, D., Cretney, W., 1974. Quantitative tar and plastic waste distributions in the Pacific Ocean. Nature 247, 31–32.
Woodall, L., Sanchez-Vidal, A., Canals, M., Paterson, G., Coppock, R., Sleight, V., Calafat, A., Rogers, A., Narayanaswamy, B., Thompson, R., 2014. The deep sea is a major sink for microplastic debris. R. Soc. Open Sci. 1 (140317), 1–8.
Yamashita, R., Tanimura, A., 2007. Floating plastic in the Kuroshio Current area, western North Pacific Ocean. Mar. Pollut. Bull. 54, 485–488.
Yoon, J.H., Kawano, S., Igawa, S., 2010. Modeling of marine litter drift and beaching in the Japan Sea. Mar. Pollut. Bull. 60, 448–463.
Zavatarelli, M., Pinardi, N., 2003. The Adriatic Sea modelling system: a nested approach. Ann. Geophys. 21, 345–364.
Zhou, P., Huang, C., Fang, H., Cai, W., Dongmei, L., Xiaomin, L., Hansheng, Y., 2011. The abundance, composition and sources of marine debris in coastal seawaters or beaches around the northern South China Sea (China). Mar. Pollut. Bull. 62, 1998–2007.
Zodiatis, G., Lardner, R., Solovyov, D., Panayidou, X., De Dominicis, M., 2012. Predictions for oil slicks detected from satellite images using MyOcean forecasting data. Ocean Sci. 8, 1105–1115.